ELSEVIER

Journal of Power Sources 99 (2001) 1–6

JOURNAL OF POWER SOURCES

www.elsevier.com/locate/jpowsour

A new composite cathode for high-performance lithium–polymer batteries

P.P. Prosini[a,b,*], C. Capiglia[a], Y. Saito[a], T. Fujieda[a],
R. Vellone[b], M. Shikano[a], T. Sakai[a]

[a] *ONRI, 1-8-31 Midorigaoka, Ikeda, Osaka 563, Japan*
[b] *ENEA, C.R. Casaccia, S. Maria di Galeria, Rome 00060, Italy*

Received 3 July 2000; received in revised form 20 September 2000; accepted 16 October 2000

Abstract

Low-molecular-weight poly(ethyleneglycol) was tested as lithium-ion conductive matrix in a crystalline V_2O_5-based composite cathode. To assess the feasibility of this composite cathode in solid-state rechargeable batteries, the ion transport properties, the chemical stability and the electrochemical stability were evaluated. The cathode exhibited fairly good electrochemical properties at a moderately high temperature. At 338 K, a ^{7}Li diffusion coefficient of about 6.8×10^{-8} cm^2 s^{-1} was measured. The cathode showed good thermal and electrochemical stability. Battery cells were assembled and their performance was evaluated at 338 K and at different discharge rates. About 270 mAh g^{-1} (corresponding to 1.8 lithium equivalents) were delivered when cycling the battery at a low discharge rate (0.04 mA cm^{-2}, *C*/24). The active material utilization decreased with increasing discharge rate. About 1.0 lithium equivalents were cycled at 0.270 mA cm^{-2}and only 0.33 at 0.480 mA cm^{-2}. © 2001 Elsevier Science B.V. All rights reserved.

1. Introduction

The poly(ethylenoxide) (PEO)–lithium salt complex has received great attention as a liquid-free solid polymer electrolyte (PE) for lithium metal-based batteries. Due to their particular structure, the PE conductivity becomes appreciable only at above ambient temperatures. The poor PE ionic transport property is the main drawback to realize high-power batteries [1]. Different causes can contribute to reduce the utilization of a cell. Depending on the cathode material properties (grain size, diffusion in the solid, porosity of the composite cathode, cathode load) and polymer electrolyte properties (diffusion in the polymer, salt concentration, thickness of the polymer electrolyte), the rate determining step can be localized in the cathode active material or in the polymer electrolyte. Newman showed that assuming a diffusion coefficient in the solid of about 5.0×10^{-11} cm^2 s^{-1}, the concentration at the surface and the average concentration in the solid are nearly identical and no concentration profiles are present in the solid. At high current density, the low rate of transport in the electrolyte phase is the main factor causing the sharp drop of the cell voltage at less than complete utilization of the cathode [2]. In the cathode compartment, the presence of the other cathode components reduces the cross-sectional area of the polymer electrolyte increasing the current density and promoting lithium depletion. Low ionic conductivity and reduced cross-sectional area lead to severe transport limitations in the depth of the electrode, thereby reducing the utilization of the active material. Newman et al. [2] have used a mathematical model to describe the dynamic behavior of lithium–polymer battery. Their model shows that the bulk of the composite cathode is at a significantly lower lithium-ion concentration with respect to the separator during cell discharge. This situation, especially in conjunction with a low cationic transference number, can adversely affect cell performance. Increasing the cell operating temperature can enhance the transport properties and the kinetics at the electrode/electrolyte interface. On the other hand, if the temperature is raised above a critical value, the electrolyte tends to decompose and unwanted corrosion and other degradation process may be accelerated.

In this work, a new composite cathode based on solid, low-molecular-weight (average $\mathrm{MW} = 2000$) poly(ethylenglycol) (PEG) was tested with respect to the ion transport properties, chemical stability and electrochemical stability. The conduction properties of the cathode and the active-material/polymer–electrolyte interface were studied at

---

[*] Corresponding author: Tel: +39-06-3048-6768;
fax: +39-06-3048-6357.
E-mail address: prosini@casaccia.enea.it (P.P. Prosini).

0378-7753/01/$ – see front matter
PII: S0378-7753(00)00654-6

various temperatures. The pulsed-field-gradient nuclear magnetic resonance (PFG-NMR) method was used to determinate the ^{7}Li and ^{19}F self-diffusion coefficients. The thermal stability of the cathode was tested by means of differential scanning calorimetry (DSC) and impedance spectroscopy (IS). Finally, solid-state batteries were assembled and cycled at various current densities, to evaluate their performance at different discharge rates.

2. Experimental

The composite cathode and the polymeric membrane were prepared by a solvent-free procedure. Samples preparation and handling were performed in a dry room (RH $< 1\%$ at 319 K). PEG (Aldrich, average MW $= 2000$) and lithium bis(trifluoromethanesulfonyl)imide (Fluka, 99%), were used as-received. The two components were weighed to give an EO/Li ratio of 20 (EO: ethylene oxide unit) and mixed in a mortar. The active material (crystalline V_2O_5, 99.99%, Rare Metallic Co. Ltd.) and the carbon (Ketjen Black, Akzo Nobel) were dried at 373 K and gently mixed in an 11:1 weight proportion. About 400 mg of this blend was added to 260 mg of the polymer–salt complex and the mixture was homogenized in the mortar. The weight fraction of the composite cathode was 55% active material, 5% carbon, 10% lithium salt and 30% PEG. The cathode was obtained by screen-printing the composite mixture onto the aluminium sheet heated at 353 K. The thickness of the electrode was about 65 μm. The geometric density of the composite cathode was about 1.0 g cm^{-3}. The polymer electrolyte was obtained by a modification of the hot-pressing technique originally proposed by Vincent and co-workers [3]. According to Kelly and co-workers, PEG was used as plasticiser to increase the solvating power of the electrolyte towards the salt at low temperatures [4]. γ-$LiAlO_2$ (Cyprus Foote Mineral Co, HAS10) was used to increase the mechanical strength of the polymer electrolyte and to improve the lithium/polymer–electrolyte interface properties [5]. PEG and the lithium salt were weighed to give an EO/Li ratio of 6 and mixed in a mortar. γ-$LiAlO_2$was dried in a dry argon atmosphere ($H_2O < 5$ ppm) at 573 K for 24 h. PEO (Aldrich, MW $= 4 \times 10^6$) was used as-received. An amount of 0.20 g of γ-$LiAlO_2$ and 0.66 g of PEO were slowly added to 0.675 g of the PEG–salt complex to form a homogeneous rubber-like mixture. The mixture was sandwiched between two Mylar sheets and placed in a hydraulic press (Grasegy/Specac Inc., P/N 15011/25011) equipped with hot plates. The sample was heated at 373 K and pressed at about 1000 N cm^{-2} for 10 min. A mechanically stable membrane with an average thickness of 150 μm was obtained. The weight fraction of the polymer electrolyte was 21% PEG, 44% PEO, 22% lithium salt and 13% γ-$LiAlO_2$. The final EO/Li ratio in the polymer electrolyte was the same as in the composite cathode. The geometric density of the polymer electrolyte was 1.4 g cm^{-3}.

Battery cells were assembled by sandwiching a polymer electrolyte disk between a lithium foil and the composite cathode. The diameter of the cathode was 0.8 cm and the weight was about 3.6 mg. The mass loading was about 4 mg of active material per cm^2. The electrochemical system was contained in stainless-steel cells. The cells were heated at 338 K in an oven and galvanostatically cycled between fixed potential values by using a battery cycler (Keisokuki, BS2500). For the utilization calculations, two equivalents of lithium per mole of vanadium pentoxide (corresponding to a specific capacity of 294 Ah kg^{-1}) were considered as the maximum capacity of the active material.

The thermal stability of the cathode was investigated with a DSC apparatus (Rigaku Thermoplus DSC 8230). The samples were prepared in dry room. The weight of the samples was of about 10 mg and they were sealed in aluminium pans. The heating rate was 5.0 K min^{-1}.

The charge transfer resistance at the polymer/active-material interface was evaluated by IS, using a frequency response analyser (NF electronic instrument, model S-5720) in the range 10 mHz–10 kHz. A polymer–electrolyte disk was sandwiched between two cathodes and this symmetrical cell was pressed between two stainless-steel current collectors. The electrodes were 65 μm thick with a diameter of 0.8 cm. The cell was tested in an oven, in the range 298–359 K.

The pulsed-field-gradient nuclear magnetic resonance (PFG-NMR) method was used to determinate the ^{7}Li and ^{19}F self-diffusion coefficients. Samples of about 3 cm height were inserted in NMR tubes (3 mm in a diameter) and the measurements were performed on a Jeol JNM-LA300WB spectrometer using a spin-echo sequence [6]. The initial echo of a magnetization vector is attenuated after applying the two gradient pulses according to the following equation:

$$M = M_0 \exp[-D(\gamma G \sigma)^2(\Delta - \tfrac{1}{3}\sigma)] \qquad (1)$$

where M_0 is the initial spin echo, D the self diffusion coefficient, γ the gyro magnetic ratio, G the strength of gradient pulse, σ the duration of gradient pulse and Δ is the time interval between the two gradient pulse. The data of ^{7}Li were acquired at a Larmor frequency of 116.8 MHz, with a 90° pulse of 8.4 ms, Δ was kept in the range 30–60 ms and σ was fixed between 1.5–3 ms. The data for ^{19}F were acquired at a Larmor frequency of 287.2 MHz, with a 90° pulse of 7.5 ms. Δ was kept in the range of 15–30 ms and σ was fixed between 1.0–3 ms. The diffusion coefficient was calculated by fitting the experimental data into the Eq. (1). The intensity of the field gradient was calibrated at 298 K using a standard sample ^{1}H in high purity D_20. The proton diffusion of standard sample is $D_{^1H} = 1.9 \times 10^{-5}$ cm^2 s^{-1}. The correspondent value obtained was 1073 Gauss cm^{-1}, which does not change effectively in the operating temperature range. For both ^{7}Li and ^{19}F, the measurements were done in the temperature range from 298 to 353 K. After each temperature increment the sample was left to thermally equilibrate for about 30 min.

3. Results and discussion

The values of the diffusion coefficient for ^{7}Li in PEG are plotted in Fig. 1 as a function of temperature. The lithium diffusion coefficient was found to range from 10^{-8} to 10^{-7} cm^2 s^{-1} in the temperature range 298–333 K. The diffusion coefficient showed an Arrhenius-type behavior consistently with other works [7,8]. From the curve in Fig. 1, the activation energy for lithium diffusion was calculated to be 46 kJ mol^{-1}.

Fig. 2 shows the apparent transference number of lithium, defined as the ratio between the ^{7}Li and the sum of ^{7}Li and ^{19}F diffusion, at various temperatures. The transference number increases by increasing the temperature up to 323 K. This behavior could be attributed to a progressive reduction of the crystallinity of PEG that occurs within this temperature range (see Fig. 3). The high value of the diffusion coefficient and the relatively high value of the transference number seem to indicate that PEG-based cathodes can be successfully used as a fast conductive matrix in the cathode of high-performance lithium–polymer batteries.

The DSC curve for the composite cathode is shown in Fig. 3. The endothermic peak at 317 K is attributed to electrolyte melting. A first exothermic peak is centred at 498 K followed by another exothermic peak at 557 K. These peaks can be related to decomposition of the polymer electrolyte in contact with the active material [9]. The decomposition process begins at about 453 K. The result shows that a PEG/V_2O_5-based cathode can be used safely at temperatures above 433 K.

The charge transfer resistance was calculated from Cole–Cole plots of the complex impedance. Fig. 4 shows the Cole–Cole plot of a symmetrical cathode/polymer–electrolyte/cathode cell under open-circuit condition at various temperatures. The semicircles have a high-frequency intercept that identifies the ionic conductivity of the polymer electrolyte. At lower frequencies, the resistance related to

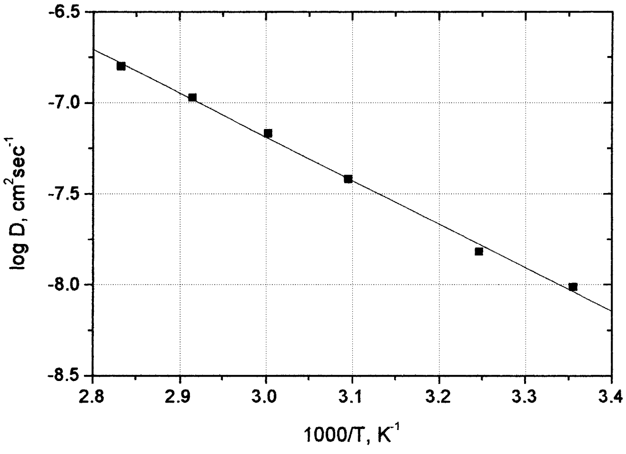

Fig. 1. An Arrhenius-plot of the ^{7}Li self-diffusion coefficient for $(CF_3SO_2)_2NLi$ in PEG for EO/Li salt ratio of 20:1.

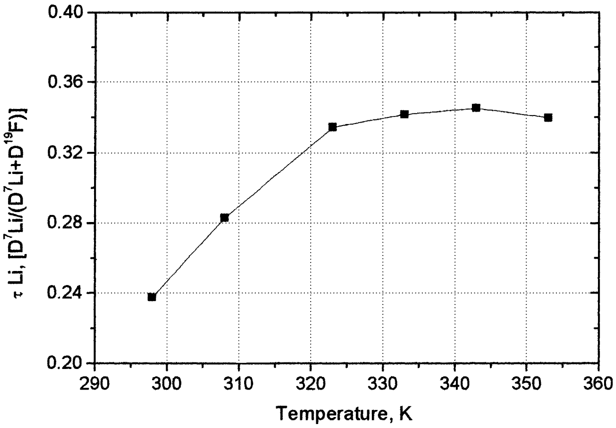

Fig. 2. The apparent transport number at various temperatures for $(CF_3SO_2)_2NLi$ in PEG for EO/Li salt ratio of 20:1. The apparent transport number was evaluated by the ^{7}Li and ^{19}F diffusion coefficients.

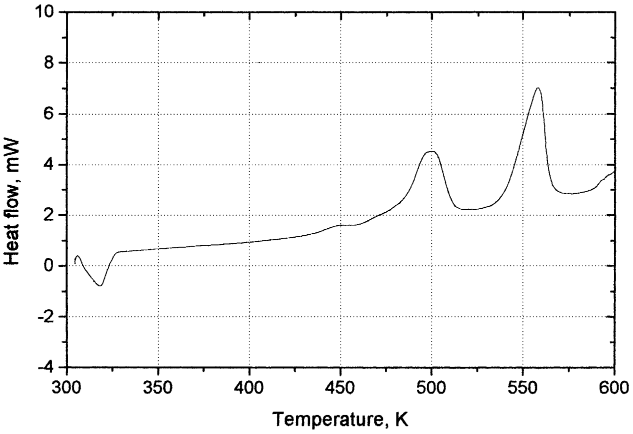

Fig. 3. DSC curve of the composite cathode. The weight fraction of the composite cathode was 55% of active material, 5% of carbon, 10% of $(CF_3SO_2)_2NLi$ and 30% of PEG.

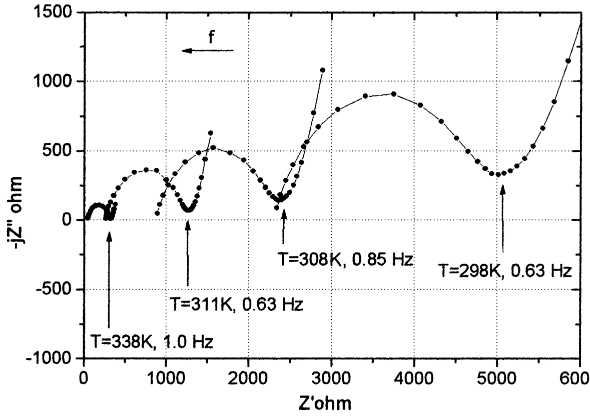

Fig. 4. Impedance spectra at various temperatures for a symmetrical cathode/polymer electrolyte/cathode cell. Frequency range: 0.1 Hz–10 kHz. Electrode surface: 0.5 cm^2.

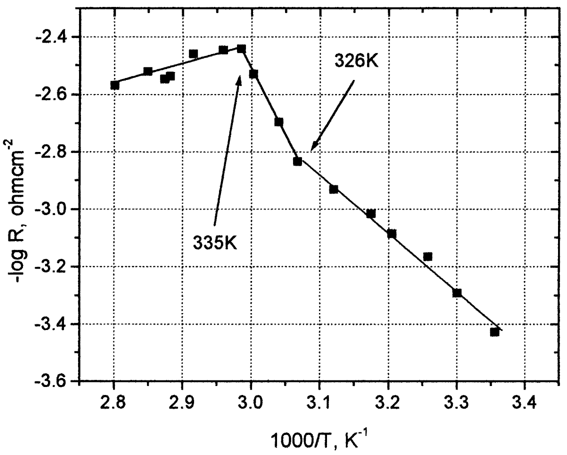

Fig. 5. An Arrhenius-plot of the charge transfer resistance. The charge transfer resistance was calculated from the Cole–Cole plots of the complex impedance. Electrode surface: 0.5 cm^2.

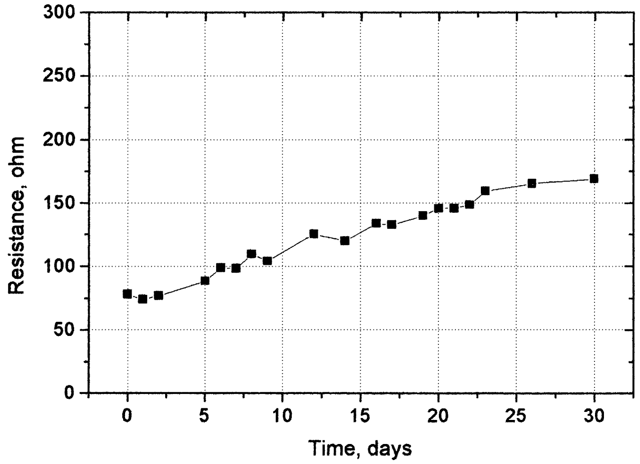

Fig. 6. Evolution of the charge transfer resistance with time for the composite cathode stored at 338 K. Data derived from the impedance analysis. Electrode surface: 0.5 cm^2.

charge transfer between the polymer electrolyte in the cathode and the active material can be identified. At very low frequencies, there is a third region in which a typical Warburg behavior, related to the diffusion of lithium ions in the cathode active material, is seen. By fitting the semiarc with a proper equivalent circuit [10], the value of the charge transfer resistance and its change with the temperature can be calculated. In Fig. 5, the charge transfer resistance is plotted versus the temperature. The charge transfer resistance showed an Arrhenius-type temperature dependence with an inflection point at about 326 K. The inflection point is related with the melting of the polymer electrolyte in the cathode compartment. The activation energy was calculated to be 38.8 and 90.2 kJ mol^{-1} before and after the cathode melting. Above 335 K, the resistance decreases with increasing temperature. For further temperature increases, the charge transfer resistance tends to increase slowly. The increase of the charge transfer resistance could be related to the growth of an insulating layer on the surface of the active material. The layer likely contains degradation products of the polymer electrolyte. The evolution of the charge transfer resistance at 338 K is shown in Fig. 6. The growth rate was about 100 ohm cm^{-2} per month. This would result in an additional voltage drop of less than 20 mV per month when discharging the cell at about 0.2 mA cm^{-2}.

In Fig. 7, the first-cycle voltage profile versus composition is shown. The lithium insertion rate was 0.08 lithium equivalents per hour. 1.0 lithium equivalent was intercalated between 3.4 and 3.2 V and another lithium equivalent was intercalated by about 2.35 V. Finally, 0.9 lithium equivalent was intercalated between 2.1 and 2.0 V. The lithium ions intercalated into the inner layer during the first intercalation process are difficult to de-intercalated because the V_2O_5 lattice has been highly and irreversibly distorted during the second intercalation [11]. About 2.3 lithium equivalents can be recovered during the following lithium de-intercalation. The charge coefficient, the ratio between the amount of charge inserted and released during the first cycle, was as high as 1.3. The specific capacity and the charge coefficient at *C*/6 rate are illustrated in Fig. 8. After the first cycle, the lithium intercalation process proceeds with high reversibility and the charge coefficient assumed the unity value. At the second discharge cycle, a capacity of about 220 Ah kg^{-1} was achieved, corresponding to about 1.5 lithium equivalents per mole of oxide. In the following cycles, a constant capacity fading affected the cell. The capacity fading was evaluated about 0.4% per cycle. The behavior upon cycling of the same active material (crystalline V_2O_5) in liquid electrolyte in the 1.9–3.4 V potential range under 0.18 mA cm^{-2} was reported by Delmas et al. [12]. In those conditions, a capacity fading of about 0.3% per cycle affected the cell. This later value does not differ too much from the value obtained by cycling the polymer electrolyte

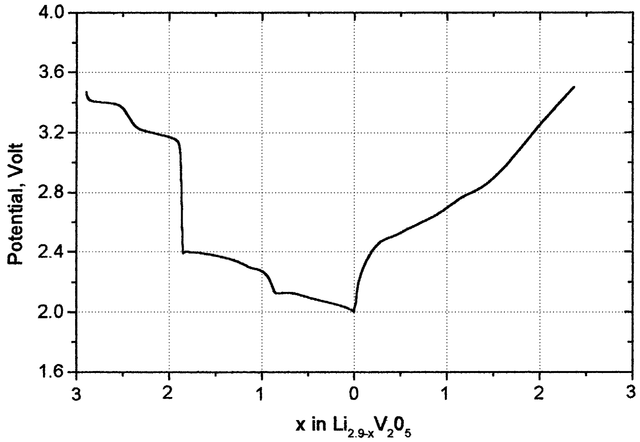

Fig. 7. Voltage profile of the first discharge/charge cycle for a V_2O_5 composite cathode/polymer electrolyte/lithium cell at 338 K. The current density was 0.04 mA cm^{-2} for charge and discharge.

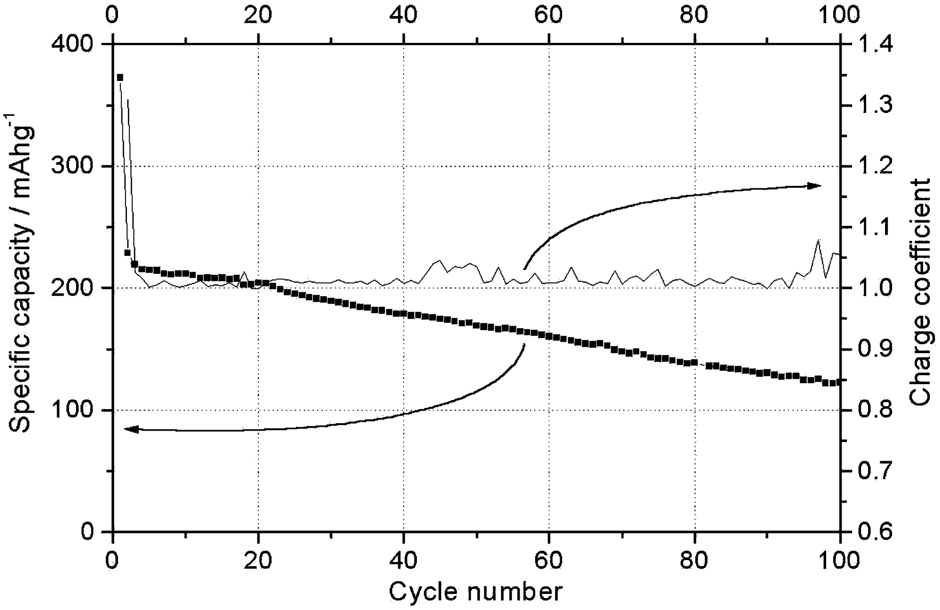

Fig. 8. Cycling behavior of a V_2O_5–PEG composite cathode/polymer electrolyte/lithium cell at 338 K. The specific capacity and the charge coefficient are plotted vs. cycle number. Discharge currents was 0.16 mA cm^{-2}. Charge current was 0.08 mA cm^{-2}.

cell. It can be concluded that the cell fading is mostly due to the irreversible structural transition of the active material and only partially due to the electrochemical system used (polymer or liquid electrolyte).

Fig. 9 shows the active material utilization as a function of discharge current density. The cell was always recharged at the same current density, to assure identical initial conditions. The utilization decreases linearly with respect to the current density. More than 1.0 lithium equivalents were cycled in about 2.3 h at 0.24 mA cm^{-2}. The active material utilization was reduced by about 17% upon doubling the discharge current. At this current density, about 51 Ah kg^{-1} were discharged in 0.36 h, delivering a specific power of about 345 W kg^{-1}, based on the weight of the active material.

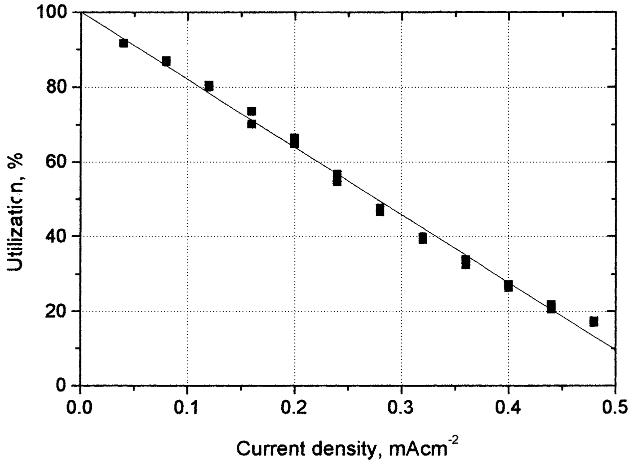

Fig. 9. Utilization of the active material for a V_2O_5 composite cathode/polymer electrolyte/lithium cell. Cut-off voltages were 2.0 V for discharge and 3.5 V for charge. The cell was discharged at different rate and charged at 0.04 mA cm^{-2}. Temperature was 338 K. The utilization was calculated considering a maximum of 2.0 equivalent per mole of V_2O_5.

The achievement of lower-temperature cell operation represents an important goal. Lower temperatures are quickly reached and easily maintained. Degradation reactions are reduced and the battery cycle life is enhanced. The performance of our prototype battery cells confirmed the promise of high utilization of the active material at moderately-low temperatures.

4. Conclusions

The transport properties and the thermal stability of a new composite cathode based on PEG/V_2O_5 were evaluated. The PFG-NMR was used to determinate the ^{7}Li and ^{19}F self-diffusion coefficients. The lithium diffusion coefficient was found to range from 10^{-8} to 10^{-7} cm^2 s^{-1} in the temperature range 298–333 K. An Arrhenius-type behavior was observed for the ^{7}Li diffusion coefficient. The calculated activation energy was 46 kJ mol^{-1}. For temperature less than 323 K, the apparent transport number was seen to increase with temperature. For further increase of the temperature, it remains stable around 0.34. DSC analysis showed that the cathode is thermally stable for temperature less than 433 K. The charge transfer resistance decreases with increasing temperature reaching a minimum at about 333 K. The charge transfer resistance at 338 K slowly increased with time. The cycling behavior of a cell was evaluated at 338 K. This cell was cycled for more than 100 cycles. The initial specific capacity was 220 Ah kg^{-1}. A capacity fading of about 0.4% per cycle affects the cells, reducing the capacity upon cycling. Battery performance was evaluated cycling with the different discharge rates. A specific capacity as high as 270 Ah kg^{-1} (corresponding to a specific energy of about 670 Wh kg^{-1}) was achieved by discharging the cell over a period of 23 h. A specific power of 345 W kg^{-1} was delivered in about 0.5 h at 0.48 mA cm^{-2}. Work is in progress to further investigate the properties of this system and to evaluate its characteristics and performance upon different cycling conditions.

Acknowledgements

The authors thank Dr. Tatsumi, Dr. H. Kataoka and Dr. Xia (who carried out the DSC analysis) for helpful discussion. Two of us (P.P.P. and C.C.) wish to thank the Science & Technology Agency of Japan for the research fellowship.

References

[1] D. Fauteux, A. Massucco, M. McLin, M. van Buren, J. Shi, Electrochim. Acta 40 (1995) 2185.
[2] M. Doyle, T.F. Fuller, J. Newman, J. Electrochem. Soc. 140 (1993) 1526.
[3] F.M. Gray, J.E. MacCallum, C.A. Vincent, Solid State Ionics 18/19 (1986) 282.
[4] I.E. Kelly, J.R. Owen, B.C.H. Steele, J. Power Sources 14 (1985) 13.
[5] F. Capuano, F. Croce, B. Scrosati, J. Electrochem. Soc. 138 (1991) 1918.
[6] E.O. Stejskal, J. Chem. Phys. 43 (1965) 3597.
[7] S. Bhattacharja, S.W. Smoot, D.H. Whitmore, Solid State Ionics 18/19 (1986) 306.
[8] W. Gorecki, R. Andreani, C. Berthier, M. Armand, M. Mali, J. Roos, D. Brinkmann, Solid State Ionics 18/19 (1986) 295.
[9] T. Shodai, B.B. Owens, H. Ohtsuka, J. Yamaki, J. Electrochem. Soc. 141 (1994) 2978.
[10] B.A. Boukamp, Solid State Ionics 20 (1986) 31.
[11] C. Delmas, H. Cognac-Auradou, J. Power Sources 54 (1995) 406.
[12] C. Delmas, S. Brethes, M. Menetrier, J. Power Sources 34 (1991) 113.